Modeling elastic properties and volume change in dental composites

P. LINGOIS, L. BERGLUND*
*Division of Polymer Engineering, Luleå University of Technology, 97 187 Luleå, Sweden
E-mail: Lars.Berglund@mb.luth.se*

A modeling approach was applied to study elastic properties and volume change in dental composites. Mechanics modeling results were compared with experimental data in model materials of known composition where the filler content was varied. Composite behavior was predicted based on polymer and filler properties in order to improve basic understanding. Model predictions agree well with data. The models were used to discuss effects of resin properties, filler volume fraction and microstructure (particle shape and filler size distribution). © *2002 Kluwer Academic Publishers*

1. Introduction
Dental composites are in principle very similar to other composite materials such as, for instance, carbon fiber/epoxy materials used in the aerospace industry. Both materials are predominantly two-phase materials; they are formed into a specific shape and then cured so that the material solidifies. The materials are then subjected to mechanical loading and chemical environments during their use. Despite of these similarities, few studies of dental composites focus on fundamental microstructural effects using a mechanics of materials approach. Instead, many studies have a direct practical objective comparing commercial materials or different restoration placement techniques with respect to performance under complex conditions.

Our long-term interest is instead to improve the basic understanding of residual stresses in dental composites, in particular the effect of microstructure and material composition. The development of predictive models is one of the major mechanics and physics challenges in this context. In residual stress predictions, it is necessary to have models for elastic properties (Young's modulus E and shear modulus G) and for the volume change s_c due to the curing reaction. The development of such models for dental composites based on particles is the primary objective of the present study.

The approach is micromechanical in nature. Because of our interest in material composition effects, parameters such as filler volume fraction, elastic constants of constituents etc. are of key importance. We are using two different approaches. In the first, semi-empirical approach, equations of simple form are investigated in order to provide easy-to-use methods for property estimates. In the second, physical approach, we compare new model composite data for E with predictions in order to improve basic understanding. We then perform a parametric study in order to estimate consequences of matrix modulus changes. Work of such nature is an important tool in the tailoring of composition in order to optimize material properties.

We have only found one previous attempt to use fundamental micromechanics models in order to predict the Young's modulus of dental composites [1]. However, the predictive capability of the models used in that study was very limited. In two other studies [2, 3], phenomenological models were used with fitting parameters. In the study by Chantler *et al.* [3] an expression for the fitting parameter was developed by comparison with numerical simulation results, thus increasing the predictive capability of this particular model.

There are several general reviews on the subject of particulate composites [4–8]. Based on those reviews, we have chosen to consider the applicability of the following models to dental composites. The Voigt and Reuss models, the three phase model [9], the Halpin–Tsai equation [10], the Lewis–Nielsen equation [11], the S-combining rule [6], the extended phenomenological model [3], the Hashin–Shtrikman bounds [12], and the composite spheres bounds [13]. The model predictions are compared with Young's modulus data generated by the preparation of model composites of different filler volume fractions (glass spheres). The matrix is a conventional light-cured methacrylate system.

A modified version of the Rosen and Hashin [14] model was used for volume change modeling.

2. Materials and methods
2.1. Composition
The resin was made of a 1:1 weight ratio mixture of Bisphenol A glycerolate (1 glycerol/phenol) diacrylate (Bis-GA) and Tri (ethylene glycol) dimethacrylate (TEGDMA). These monomers proportions were chosen because it gives a low viscosity mixture and because the composition is the same as in the commercial composite Z100. The photoinitiator system was based on a

---

*Author to whom all correspondence should be addressed.

mixture of camphorquinone (CQ) with a molar ratio of 6×10^{-2} and N,N-dimethyl-p-toluidine (DMPT) with a molar ratio of 6×10^{-3}. All chemical products were provided by Sigma-Aldrich Chemicals and used as received. The filler was Spheriglass® from Potters and Ballotini, grade 5000 (solid glass spheres, mean diameter 3.5–7 microns, silanised for acrylate systems).

Since the maximum filler content is limited with our materials and techniques, a commercial composite Z100 from 3M was used in order to have one material with a higher filler content. This composite was chosen since it is based on a similar resin system as ours. The particles have an aspect ratio close to one and rounded edges as observable in an SEM micrograph in the Technical product profile of Filtek™ Z250 from 3M [15].

2.2. Specimen preparation

The composite mixture was degassed at room temperature to remove air. Then it was poured in a Teflon mould with the following dimensions: $1 \times 13 \times 50$ mm. Mylar® films were placed on top and bottom of the mould. The sample was light cured with a lamp Dulux S/E 9 W/71. It is not a common dental lamp, its primary application is for the curing of paints and adhesives. It has the advantage of being able to cover an area of 30×100 mm and it has a high output spectrum in the blue range (400–500 nm) as in dental lamps. One face of the samples was irradiated for 7 min at a distance of 1 cm and then the second face was irradiated under the same conditions. The commercial composite was just pressed in the mould and then light cured under the same conditions as previously described. After measurement of the density, using a liquid displacement technique, a strain gauge (CEA-06-240UZ-120) from Measurements Group was bonded to the specimen in order to measure strain in the loading direction.

In order to determine the Poisson's ratio of the pure resin, the samples were made in a Teflon® mould with the dimensions: $1 \times 24 \times 230$ mm. They were then cured 7 min on each side as previously. A strain gauge (CEA-06-240UZ-120) was bonded to the specimen in order to measure strain in the transverse direction.

2.3. Shrinkage

The volume change, s, was determined by the following relationship:

$$s = \frac{d_{\text{cured}} - d_{\text{uncured}}}{d_{\text{cured}}} \times 100 \qquad (1)$$

where d is the density. A positive value denotes contraction.

The density of the uncured material was estimated from the density of the different constituent products, with the assumption that there is no interaction.

The density of the cured system was determined using a water displacement technique as described in ASTM D792 (1991). The samples were less than one minute in the water, so water sorption could be neglected.

2.4. Mechanical properties

The Young's modulus measurements were carried out in a Polymer Laboratories miniature materials tester at a strain rate of around 1%/min. The strain gauge is connected to a quarter Wheatstone bridge of an amplifier. The data are then converted from analog to digital and saved in a computer with the load data.

The Poisson's ratio measurements were carried out in an Instron machine with a 500 N load cell. A 50 mm extensometer was used to measure the extension in the loading direction, a strain gauge for the transverse contraction. The extensions and the load data were saved on a computer as previously.

2.5. Temperature

The increase of temperature during curing was measured by placing a 1 mm thick model composite layer on an aluminum plate with the dimensions $20 \times 70 \times 1$ mm. A thermocouple was fixed on the other side of the aluminum plate. The sample was cured and the temperature was recorded during curing.

3. Modeling

In the present study, we are interested in two models. The first is a model for the elastic properties of a dental composite based on stiff particles in a softer matrix. The second is a model for volume change in the composite as the matrix is shrinking or expanding.

For an isotropic material, there are three elastic constants, the Young's modulus E the shear modulus G and the Poisson's ratio ν. Only two of the constants are independent:

$$G = \frac{E}{2(1 + \nu)} \qquad (2)$$

We choose two approaches. The first we call a semi-empirical approach where the intention is to have a simple model in order to estimate elastic constants. The second we call the physical model approach. In this case, the models are based on elasticity theory. Because of the nature of these models, it becomes possible to interpret reinforcement mechanisms on a physical basis.

The second case considered is volume change in the composite. Regardless of the reason for volume change, in the modeling perspective, this is analogous to a thermal expansion problem. This problem is easier to solve than the elastic property problem. Hashin and Rosen [14] reviewed the case of a statistically homogeneous two-phase composite. The solution is based on elasticity theory and a physical model.

3.1. Elastic constants
3.1.1. Semi-empirical models

These expressions are based on some physics arguments although fitting parameters are included. Several of the most widely used semi-empirical models are based on an expression of the following form, as

discussed by McGee and McCullough [6]:

$$P_c = \frac{P_m(1 + \xi \chi V_f)}{1 - \chi \psi V_f}$$

$$\chi = (P_f - P_m)/(P_f + \xi P_m) \qquad (3)$$

where P is the bulk modulus (K) or the shear modulus (G), V_f is the filler volume fraction, the subscripts: c, m, f refer to the composite, the matrix, and the filler respectively. ξ and ψ are parameters specifically defined in each model, this is the difference between individual models. The Young's modulus and the Poisson's ratio are related to the bulk and shear modulus by the following relationships:

$$E = \frac{9KG}{3K + G}$$

$$\nu = \frac{3K - 2G}{2(3K + G)} \qquad (4)$$

There are several specific cases of this approach which differ only in the way ξ and ψ are determined.

3.1.1.1. Lewis and Nielsen model: Lewis and Nielsen [11] used an analogy with the Mooney equation for viscosity of suspensions. They proposed a modification of the Kerner equation [16], to account for the limits imposed by the maximum packing for uniformly sized spherical particles. The expressions for the parameters introduced in Equation 3 are:

$$\xi_K = \frac{2(1 - 2\nu_m)}{1 + \nu_m}$$

$$\xi_G = \frac{7 - 5\nu_m}{8 - 10\nu_m}$$

$$\psi = 1 + \left(\frac{1 - V_f^{max}}{\left(V_f^{max}\right)^2}\right) V_f \qquad (5)$$

where V_f^{max} is the maximum volume fraction of the filler. The parameter ξ is different for the bulk and the shear modulus; subscripts K and G refer to the bulk modulus and the shear modulus respectively.

3.1.1.2. S-mixing rule: Another classical approach is the S-mixing rule [6]. In the case of rigid, uniformly sized spheres, the parameters are:

$$\xi_K = \frac{2(1 - 2\nu_m)}{1 + \nu_m}$$

$$\xi_G = \frac{7 - 5\nu_m}{8 - 10\nu_m}$$

$$\psi = 1 + \left(\frac{1 - V_f}{V_f^{max}}\right)\left(V_f V_f^{max} + (1 - V_f)(1 - V_f^{max})\right)$$

$$(6)$$

For both models (Equations 5 and 6), the parameter V_f^{max} needs to be determined. For uniformly sized spheres, V_f^{max} is 0.66 for random packing. Since dental

composites do not consist of uniformly sized particles, V_f^{max} can be between 0.66 and 1. In the case of a given commercial material with non-uniform particle size, it is not straight-forward to determine V_f^{max}.

3.1.1.3. Halpin–Tsai model: The Halpin–Tsai equation was first developed to predict the transverse Young's modulus of continuous fiber composites [17]. For both the case of transverse composite modulus and the case of particulate composites, P in Equation 3 represents the Young's modulus and ψ equals 1. Values for ξ were then obtained by fitting the results of detailed numerical analyses. It was found that $\xi = 2$ for particulate filled systems. In the same manner, it was found that $\xi = 1$ for the shear modulus. The Halpin–Tsai equations have a simple form and are based on numerical modeling of a real physical problem although effects from matrix Poisson's ratio are neglected in the final expressions. In our particular case, the final Halpin–Tsai expressions used in order to predict the elastic properties of dental composites are:

$$E_c = \frac{E_m\left(1 + 2\dfrac{E_f - E_m}{E_f + 2E_m} V_f\right)}{1 - \dfrac{E_f - E_m}{E_f + 2E_m} V_f}$$

$$G_c = \frac{G_m\left(1 + \dfrac{G_f - G_m}{G_f + G_m} V_f\right)}{1 - \dfrac{G_f - G_m}{G_f + G_m} V_f} \qquad (7)$$

The Poisson's ratio depends on G and E according to:

$$\nu = \frac{G}{2E} - 1 \qquad (8)$$

3.1.1.4. Chantler et al. model: Chantler *et al.* [3] present a phenomenological model based on the classic Hertzian elastic contact theory. In this case, the expression is the following:

$$E_c = E_m(E_f/E_m)^{1-(1-V_f)^\beta} \qquad (9)$$

The parameter β was determined by fitting Equation 9 to numerical simulation results for uniformly sized spherical particles [18]. The resulting empirical expression is the following:

$$\beta = \frac{2\left[\left(1 - \nu_f^2\right)/\left(1 - \nu_m^2\right)\right]^{1.7}}{\ln(E_f/E_m)} \qquad (10)$$

where ν_f and ν_m are the Poisson's ratio of the filler and matrix respectively. It is interesting to note that Bush [17] found a significant effect from ν_m.

3.1.2. Physical models
3.1.2.1. Rule of mixture: The simplest physical models are based on assumptions of uniform stress (Reuss) or strain (Voigt) in both constituents (matrix and filler). These models are commonly termed rule of mixtures.

The results are presented as upper (Voigt) and lower (Reuss) bounds to, for instance, E as a function of V_f. As pointed out by Hill [19], none of the models based on uniform stress or uniform strain fields can be strictly correct: the interfacial forces are not in equilibrium for constant strain; interfacial discontinuities must exist for constant stress.

3.1.2.2. Hashin–Shtrikman model:
The Hashin–Shtrikman model [12] is based on variational analysis. Also for this model, two different assumptions lead to an upper and a lower bound. The bounds are obtained without any information regarding filler shape or size. However, in the case of a large modulus mismatch between the resin and the filler, the bounds are far apart from each other.

3.1.2.3. Composite spheres model:
Hashin [13] developed the composite spheres (CS) model which considers particulate filled systems with a specific, broad distribution of particle size, with a size range extending down to infinitesimal particles. The model is again based on variational analysis with rigorous assumptions and does not contain any fitting parameters. However, because of the assumptions involved, single sized particle composites of high filler concentrations are not expected to be well described by this model. An exact analytical expression is available for the bulk modulus, this corresponds to the lower bound of the Hashin–Shtrikman model. For the shear modulus, upper and lower bounds are obtained. The expressions are:

lus of the CS model corresponds to the lower bound of the Hashin–Shtrikman model. The CS bounds are much closer to each other than in the Hashin–Shtrikman model. However, the model does not properly describe the shear loading case.

3.1.2.4. Generalized self-consistent scheme:
The generalized self-consistent scheme (SCS) reported by Christensen and Lo [9] was developed in order to obtain a better description of the shear loading case. In this model an inclusion of radius a is embedded in a sphere of matrix material with a radius b. The ratio $\eta = a^3/b^3$ is taken to be equal to the volume fraction of filler. However, the choice of η can be argued, as did Hashin [20]. The composite sphere is embedded in a medium that is assigned the unknown effective properties of the filled material. This model gives the same expression for the bulk modulus as the CS model, but it gives an exact analytical solution for the shear modulus. The solution is between the CS model bounds but of complex form, see McGee and McCullough [6]. From the theoretical point of view, the SCS model contains a better description of the shear loading case as compared with the CS model.

3.1.3. Volume change
The volume change problem is treated like a thermal expansion problem. Rosen and Hashin [14] presented a model for the coefficient of thermal expansion α which takes residual stresses into account. For instance, if the

$$K_c = K_m + \frac{V_f(K_f - K_m)}{1 + (1 - V_f)\left[(K_f - K_m)\Big/\left(K_m + \frac{4}{3}G_m\right)\right]}$$

$$G_- = G_m + \frac{V_f}{1/(G_f - G_m) + 6(1 - V_f)(K_m + 2G_m)/5G_m(3K_m + 4G_m)}$$

$$G_+ = G_m\left[\frac{V_f}{1/(\gamma - 1) + A(1 - V_f) - V_f\left(1 - V_f^{2/3}\right)^2\Big/\left(BV_f^{7/3} + C\right)}\right] \quad (11)$$

with

$$\gamma = G_f/G_m$$

$$A = \frac{2(4 - 5\nu_m)}{15(1 - \nu_m)}$$

$$B = \frac{10(1 - \nu_m)}{21}$$
$$\times \frac{(7 - 10\nu_f)(7 + 5\nu_m) - \gamma(7 - 10\nu_m)(7 + 5\nu_f)}{4(7 - 10\nu_f) + \gamma(7 + 5\nu_f)}$$

$$C = \frac{10}{21}(7 - 10\nu_m)(1 - \nu_m)$$

The bounds for G are converted to bounds for E using Equation 4. The lower bound of the shear modu-

matrix expands and the filler is rigid with no expansion, significant local stresses are formed in the matrix. Their solution for thermal expansion in the case of a macroscopically isotropic composite (like any dental composite) is:

$$\alpha_c = \alpha_f + \frac{(\alpha_m - \alpha_f)}{(1/K_m - 1/K_f)}\left[\frac{1}{K_c} - \frac{1}{K_f}\right] \quad (12)$$

where the subscripts c, m, and f refer to the composite, matrix, and inclusion respectively. K_c is the composite bulk modulus expressed in Equation 11.

In a modeling perspective, the reason for constituent volume change is not important. Therefore, in the case of matrix shrinkage, we can apply the same expression as in Equation 12, assuming that α_f equals zero. Thus

the expression for composite shrinkage (s) is:

$$s_c = \frac{s_m}{(1/K_m - 1/K_f)}\left[\frac{1}{K_c} - \frac{1}{K_f}\right] \qquad (13)$$

with designations as in Equation 12.

We also use predictions from a simplistic model where the shrinkage s_c is assumed to depend linearly on the matrix shrinkage according to

$$s_c = s_m(1 - V_f) \qquad (14)$$

4. Results and discussion

The experimental data used in model predictions are presented in Table I.

We conducted experiments where the final composite shrinkage s_c of the material due to the curing reaction was determined based on density measurements. The volume fraction of filler was varied, whereas the light intensity and the curing time were the same for all materials. Fig. 1 compares the experimental data for s_c as a function of V_f with the theoritical model predictions. According to the Rosen and Hashin model, s_c decreases in a non-linear way with V_f. The reason is that residual stresses form in the matrix. Shrinkage of the soft matrix is constrained by the stiff filler particles. The model predictions show good agreement with data at high filler content, whereas the discrepancies are larger at low filler content.

Part of the reason for this is related to the fact that there is an increase in temperature in the material during curing. The maximum temperatures measured during curing were 55, 45, 43, 40, and 38°C for 0, 7, 16.5, 40, 55 volume % of filler content, respectively (higher temperature for lower filler content). A consequence of

TABLE I Material data used in the models. The number in parentheses is the standard error

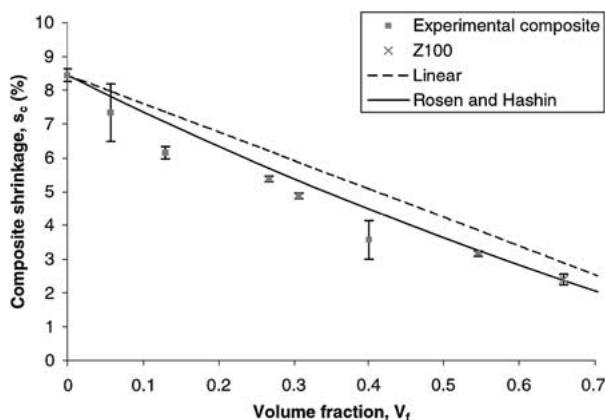|	
Matrix Young's modulus, E_m (GPa)	2.9 (±0.2)
Matrix Poisson's ratio, ν_m	0.37 (±0.02)
Matrix shrinkage, s_m(%)	8.45 (±0.08)
Filler Young's modulus, E_f (GPa)	72
Filler Poisson's ratio, ν_f	0.22

Figure 1 Composite shrinkage s_c as a function of V_f. The bars represent the standard error and the lines are modeling predictions.
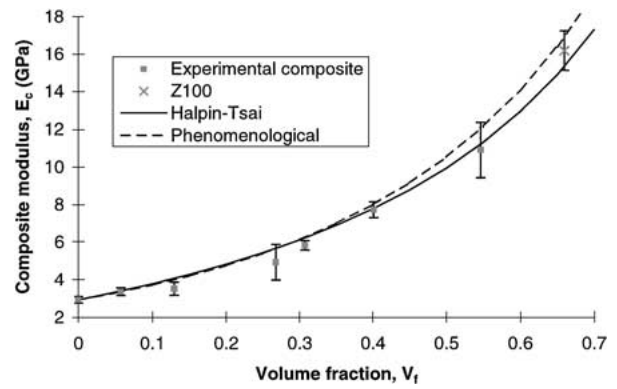

Figure 2 Composite modulus E_c as a function of V_f. The bars represent the standard error and the lines are semi-empirical modeling predictions.

these temperature differences and radiation shielding due to particles is that the degree of cure will be lower in composites than in the neat resin. Therefore, the resin shrinkage is also lower in the composites. This is why experimental data are lower than predictions at low V_f. At higher V_f, the shrinkage in the resin is still smaller as compared with the neat resin. However, the volume of resin in the composite is so small that the discrepancies between data and predictions become smaller at high V_f. Note the low shrinkage of Z100 due to its high V_f ($V_f = 0.66$).

For comparative purposes, the linear relationship of Equation 14 is presented in Fig. 1. The difference as compared with the Rosen and Hashin model is significant. Clearly, the effect of residual stresses has to be taken into account in the prediction of s_c.

The next problem is finding a predictive semi-empirical model for elastic constants of dental composites. Such a model has a simple form and can be readily used to estimate elastic constants of dental composites based on various matrices and fillers. In Fig. 2, experimental data for Young's modulus are presented as a function of V_f. There is a non-linear increase in E with V_f. We may also note that E increases quite strongly from about 11 GPa to about 16 GPa as V_f goes from 0.55 to 0.66. Among the semi-empirical models discussed in the modeling section, only predictions from Halpin–Tsai and the Chantler *et al.* model are presented. The reason is that the Lewis–Nielsen and the S-combining rule both require fitting parameters to be determined from experimental data. Even with the fitting procedures, those models still gave large discrepancies between predictions and data.

The Halpin–Tsai model and the Chantler *et al.* model both have fitting parameters determined from numerical analysis. No experimental calibration is needed and their predictive capability is very good. In addition, both models provide good agreement with the present experimental data.

In the work by Bush [17], on which the Chantler *et al.* model is based, predictions also overestimated experimental data. On the other hand, McGee and McCullough [6] stated that Halpin–Tsai predictions tend to understimate the Young's modulus at high V_f, which is also the case here. Since predictions from both models are rather close, our data are insufficient to
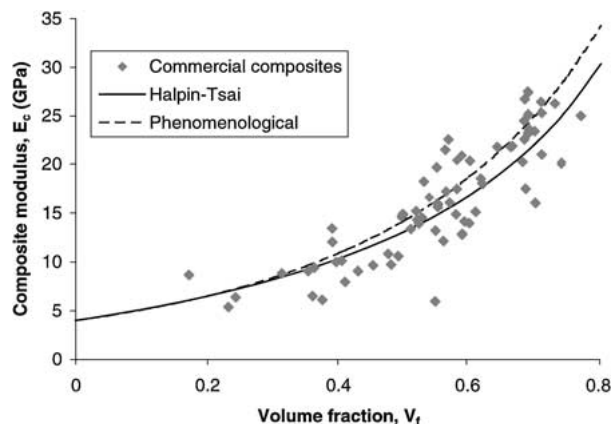
Figure 3 Composite modulus E_c as a function of V_f, experimental data from Willems *et al.* [22] for commercial dental composites. Lines represent semi-empirical modeling predictions.

Figure 5 Composite modulus E_c as a function of V_f. Data are for non-spherical fillers [20]. Lines represent modeling predictions as in Fig. 4.

decide on the best model because of the experimental scatter. Any of the two models can be recommended.

In Fig. 3, experimental data from numerous commercial dental composites are presented. Chantler *et al.* model again predicts slightly higher modulus than the Halpin–Tsai model at high V_f. The large scatter in the data is a consequence of the large variation in filler types and shapes, matrix properties and possibly also uncertainties in the measurements. This illustrates that uncertainties regarding filler shape, matrix modulus, and similar factors are more important than the selection of Halpin–Tsai or Chantler *et al.* model.

The next problem to consider is the comparison between data and predictions using physical models. Here the objective is to improve our understanding of the mechanisms of reinforcement and the roles of the constituents. In Fig. 4, E is again plotted as a function of V_f. Predictions using Voigt, Reuss, and Hashin–Shtrikman models are not presented. The reason is that the disagreement with experimental data is substantial, as was discussed by Katz [1].

In Fig. 4, the SCS model predictions fall between the CS upper and lower bounds. Due to the problem with the CS model for shear loading (see modeling section), we focus on the SCS predictions. Agreement with experimental data is remarkably good, considering the lack of any fitting parameter. However, at high V_f, data
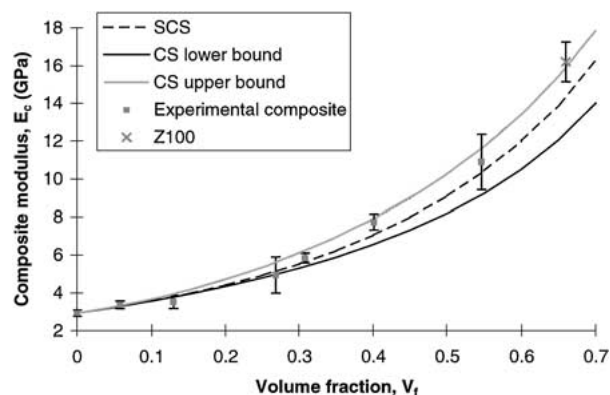
tend to be higher than predictions. SCS models have also previously been observed to underpredict properties at high V_f [6, 8]. Nemat–Nasser *et al.* [8] found that experimental data for shear viscosity (similar problem as shear modulus) depended on particle size distribution at high V_f. The maximum packing V_f is assumed to be close to 1 in the SCS model. It is possible that the maximum packing V_f is perhaps 0.7 for the particle size distribution in our material and in Z100. For this reason, some discrepancies between SCS predictions and data are expected at high V_f.

In many commercial materials, the filler particles are non-spherical. Braem *et al.* [21] provided data for such a material where the particles were ground and therefore not spherical. In Fig. 5, those data are compared with predictions from the SCS and the CS upper bound models. Non-spherical particulate composites have slightly higher E than those based on spherical particles. From Fig. 5, we can conclude that the CS upper bound model predictions agree well with data. In the predictions, a Poisson's ratio of 0.36 was used for the polymer matrix as was assumed in Chantler *et al.* [3]. When we instead used a Poisson's ratio of 0.385, the agreement between CS upper bound and data was even better. Predictions are quite sensitive to matrix Poisson's ratio and either this property or G therefore need to be determined experimentally.

In order to illustrate the application of predictive models we may consider the question of matrix modulus effects on composite modulus. Lowering of matrix

Figure 4 Composite modulus E_c as a function of V_f. The bars represent the standard error, lines represent predictions from physical models, SCS: generalized self-consistent scheme, CS: composite spheres model.
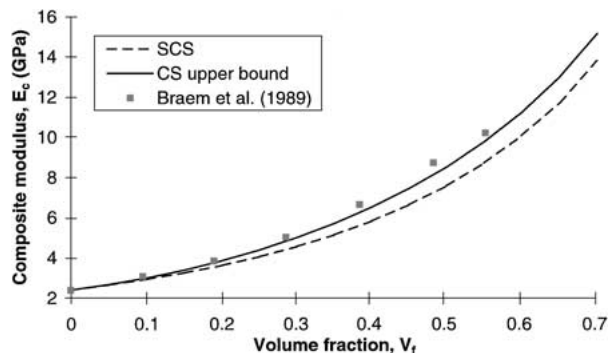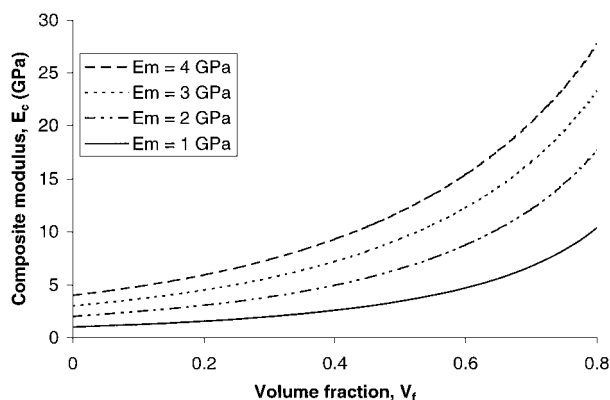

Figure 6 Predicted composite modulus E_c as a function of V_f for different values for E_m, matrix modulus. Predictions are based on the generalized self-consistent scheme.

modulus has been suggested to reduce residual stresses in dental restorations (provided all other parameters are unchanged). In Fig. 6, we present predictions for matrix effects on the composite modulus, using the SCS model. Effects are quite strong. For instance, as the matrix modulus is decreased from 4 GPa to 2 GPa (a realistic possibility), the composite modulus at $V_f = 0.6$ decreases from 15.4 to 8.7 GPa. Therefore, reduced matrix modulus is really a possible route to reduced residual stresses in dental restorations.

5. Conclusions

Existing micromechanical models were compared with data for dental composites of different filler volume fraction V_f. For volume change predictions, the Rosen–Hashin model predictions agreed well with data. The importance of filler-matrix interaction was demonstrated since a simplistic linear model overpredicted composite shrinkage.

The semi-empirical Halpin–Tsai and Chantler *et al.* equations were suggested as a convenient tool for prediction of elastic constants in dental composites (Equations 7—10). Predictions of Young's modulus for the composite, E_c, showed good agreement with data at different V_f. Modeling using the more physics based generalized self-consistent scheme (SCS) was used to improve understanding of microstructural effects on E_c. At high V_f, SCS modeling may underpredict experimental data. A possible cause is that, in this model, the maximum packing V_f^{max} is assumed to be close to 1. Finally, as the SCS model was applied, the effect of matrix modulus E_m on E_c was found to be significant. Provided matrix shrinkage and other aspects are not adversely influenced, a matrix system with lowered E_m could therefore be a practical route to lowered residual chemical stresses.

References

1. J. L. KATZ, *J. Mater. Sci. Lett.* **7** (1988) 133.
2. M. BRAEM, V. E. VAN DOREN, P. LAMBRECHTS and G. VANHERLE, *J. Mat. Sci.* **22** (1987) 2037.
3. P. M. CHANTLER, X. HU and N. M. BOYD, *Dent. Mater.* **15** (1999) 144.
4. T. G. RICHARD, *J. Comp. Mater.* **9** (1975) 108.
5. J. C. SMITH, *J. Res. Nat. Bur. Stand. Section A, physics and chemistry* **80A** (1976) 45.
6. S. H. McGEE and R. L. McCULLOUGH, *Polym. Compos.* **2** (1981) 149.
7. R. M. CHRISTENSEN, *J. Mech. Phys. Solids* **38** (1989) 379.
8. S. NEMAT-NASSER, N. YU and M. HORI, *Mech. Mater.* **15** (1993) 163.
9. R. M. CHRISTENSEN and K. H. LO, *J. Mech. Phys. Solids* **27** (1979) 315.
10. J. C. HALPIN and S. W. TSAI, Air Force Technical Report AFML-TR-67-423,1969.
11. T. B. LEWIS and L. E. NIELSEN, *J. Appl. Polym. Sci.* **14** (1970) 1449.
12. Z. HASHIN and S. SHTRIKMAN, *J. Mech. Phys. Solids* **11** (1963) 127.
13. Z. HASHIN, *J. Appl. Mech.* **29** (1962) 143.
14. B. W. ROSEN and Z. HASHIN, *Int. J. Eng. Sci.* **8** (1970) 157.
15. 3M Dental Products Laboratory, in "Filtek™ Z250 Universal Restorative System," Technical Product Profile from 3M, Saint Paul, MN, USA, 1998.
16. E. H. KERNER, *Proc. Phys. Soc.* **69B** (1956) 808 as quoted in S. McGEE and R. L. McCULLOUGH, *Polym. Comp.* **2** (1981) 149.
17. J. W. ASHTON, J. C. HALPIN and P. H. PETT, in "Primer on Composite Materials: Analysis" (Technomic, Stamford, Conn., 1969).
18. M. B. BUSH, *Mater. Sci. Eng.* **A 154** (1992) 139.
19. R. J. HILL, *J. Mech. Phys. Solids* **12** (1964) 199.
20. Z. HASHIN, *J. Appl. Mech.* **50** (1983) 481.
21. M. BRAEM, W. FINGER, V. E. VAN DOREN, P. LAMBRECHTS and G. VANHERLE, *Dent. Mater.* **5** (1989) 346.
22. G. WILLEMS, P. LAMBRECHTS, M. BRAEM, J. P. CELIS and G. VANHERLE, *ibid.* **8** (1992) 310.